Cell Tissue Res (2010) 339:597–611
DOI 10.1007/s00441-009-0912-9

REGULAR ARTICLE

Haemostatic and immune role of cellular clotting in the sipunculan *Themiste petricola*

Victoria Cavaliere · Daniela L. Papademetrio · Elida M. C. Alvarez · Guillermo A. Blanco

Received: 3 September 2009 / Accepted: 20 November 2009 / Published online: 1 February 2010

Abstract Sipunculans, a small phylum of coelomated marine worms closely related to polychaete annelids, lack a true circulatory system. We have previously shown that the sipunculan *Themiste petricola* can form a cellular clot, without congealing, of cell-free coelomic fluid. The clot is formed by the aggregation of large granular leukocytes (LGLs) and may serve not only haemostatic but immune functions, since dissimilar particles may become entrapped within it. We have now evaluated the capacity of a massive clot, induced in vitro by sea water contact, to stop coelomic fluid flow. We have further studied smaller clots induced on glass-slides either with or without the presence of bacteria placed for entrapment within the clot. The fate of clotting LGLs is cell death while forming a cohesive mass, although cytoplasmic and nuclear remnants are shed from the clot. These remnants and any bacteria that avoid clot entrapment or are detached from the clot are engulfed by non-clotting cells that include small granular leukocytes (SGLs) and large hyaline amebocytes (LHAs). Both cell types can be found other than in the clot but SGLs also occur around the clot edges heavily loaded with engulfed material. The cytoskeletal arrangement of SGLs evaluated with phalloidin-rhodamine correspond to motile cells and contrast with that of clotting LGLs that form a massive network of F-actin. Thus, the complementary roles between clotting LGLs and non-clotting SGLs and LHAs act a central immune strategy of *Themiste petricola* to deal with body wall injury and pathogen intrusion into the coelomic cavity.

Keywords Coagulation · Immunity · Cell death · Microparticles · Sipuncula · *Themiste petricola* (Sipunenlida)

Introduction

The clotting system has been extensively studied in invertebrates with open circulatory systems such as insects and crustaceans (Bohn 1986; Gregoire 1951). Clot formation involves the congealing of cell-free haemolymph by means of the rapid activation of coagulogen protein (Osaki and Kawabata 2004; Solum and Murer 2007; Theopold et al. 2004). Coagulocytes also participate in clot formation in insects and crustaceans but the humoral component appears to be more relevant in creating a hard clot (Gregoire and Goffinet 1979; Jiravanichpaisal et al. 2006). Resistance conferred by a hard clot is critical to prevent the loss of haemolymph because of the positive pressure required for haemolymph circulation and the presence of a rigid exosqueleton (McMahon et al. 1997; Ratcliffe and Gagen 1977; Rowley and Ratcliffe 1976). Coagulocytes have an accessory role in the formation of a soft clot and have been found in low numbers interspersed within the mesh created by the humoral components of the clot (Theopold et al. 2002). These cells are activated after the initiation of coagulation and are later disintegrated with their remnants becoming an integral part of the clot (Bidla et al. 2005; Scherfer et al. 2004). The process of coagulocyte death

This work was supported by CONICET Grant PEI 6377 (to G.B.).

V. Cavaliere · D. L. Papademetrio · E. M. C. Alvarez · G. A. Blanco (✉)
Department of Immunology,
IDEHU-National Research Council (CONICET),
School of Pharmacy and Biochemistry,
University of Buenos Aires (UBA),
Junin 956 4to piso,
Capital Federal 1113 Buenos Aires, Argentina
e-mail: gblanco@ffyb.uba.ar

within the clot after activation shares some features with eukaryotic cells undergoing apoptotic cell death, such as the exposure of phosphatidylserine at the external membrane leaflet (Schmidt and Theopold 1997).

Sipunculans are a small phylum of non-segmented coelomated marine worms. Recent molecular phylogenetic analyses suggest a close relationship between Sipuncula and the phylum Annelida, particularly with the major group Polychaeta, which includes mostly marine worms (Dunn et al. 2008; Struck et al. 2007). On the basis of these studies, Sipuncula have been proposed as belonging within Annelida (Struck et al. 2007). A recent study in the sipunculan *Phascolosoma agassizii* has found a segmental mode of neural patterning similar to that of annelids (Kristof et al. 2008). Sipunculans lack a true circulatory system (Hyman 1959; Schulze et al. 2007). The pressure of the fluid contained in the coelomic cavity depends on the contraction of muscles of the body wall and the introvert (Rice 1993). Relaxation of the body wall muscles can lower intracoelomic pressure to values close to that of the surrounding sea water. The term clot is commonly used to denote the formation of a haemostatic soft mass in a fluid such as blood or haemolyph and has been used a synonym for the congealing of cell-free fluid since William Hewson showed, in the 18th century, that blood coagulation is attributable to the clotting of plasma rather than changes in the cellular constituents (Doyle 2006). However, clotting in sipunculans does not involve the congealing of cell-free coelomic fluid (Blanco 2007; Blanco et al. 2008; Dybas 1976; Towle 1975). Instead, these worms have a peculiar mechanism of preventing the loss of coelomic fluid under conditions of body wall injury that may open a breach into the surrounding sea water. This mechanism consists of the formation of a cellular clot resulting from the homotypic aggregation of a coelomic cell subtype designated large granular leukocytes (LGL; Blanco et al. 2008).

In Sipuncula, cellular aggregation occurs rapidly when coelomic fluid comes into contact with sea water. This cellular clot is not gel-like and only aggregated cells have been observed to be an integral part of its structure; however, it may be resistant enough to prevent the loss of coelomic fluid at low intracoelomic pressures. Clotting in sipunculans appears to be not only a haemostatic mechanism, but also a central immune response. Thus, the homotypic aggregate that forms the clot might be able to entrap many kinds of foreign particles. The aggregation and activation of LGLs appears to be superseded by a process of cell death within the clot, whereby the mass of aggregated and additional dead cells become a large haemostatic plug. Nevertheless, during clot formation, cytoplasmic and nuclear fragments from LGLs may be shed from the clot (Blanco 2007; Blanco et al. 2008).

Our previous observations of the sipunculan *Themiste petricola* have suggested that the clot, either with or without entrapped foreign particles, is connected to phagocytic cells acting as scavengers of material shed from the clot. We have proposed that material phagocytosed by these cells might include either self-derived nuclear and cytoplasmic remnants of LGLs or foreign particles entrapped within the clot (Blanco et al. 2008). The aims of this study have been to explore the dual haemostatic-immune implication of clot formation, to characterize the formation and distribution of LGL-derived cytoplasmic and nuclear remnants shed from the clot and to characterize the non-dying clot-associated cells, i.e. small granular leukocytes (SGLs) and large hyaline amebocytes (LHAs), as two different phagocytic cell types actively involved in removing remnants of LGLs.

Materials and methods

Worms

Adult *Themiste petricola* were collected from crevices in intertidal rocks at Santa Elena beach on the coast of Argentina (34°S latitude) and maintained in 500-ml plastic boxes with frequently renewed filtered sea water with 32 parts per thousand (ppt) salinity at 18°C. The salinity of the sea water that the subject worms were originally found in was 32 ppt. Prior to harvesting coelomic fluid, the worms were passed through 0.4 M NaCl to wash out the sea water adsorbed to the body wall. The NaCl solution was adjusted to 0.4 M to resemble the concentration of these ions in *Themiste petricola* coelomic fluid (Blanco et al. 1995).

Criteria used to distinguish sipunculan immune cells

The coelomic cavity of sipunculans contains a number of cell types involved in respiration (haemerythrocytes or red cells), reproduction (ovocytes or spermatozoids depending on the sex of the worm) and the immune response (LGLs, LHAs and SGLs). LHAs were identified as being large leukocytes of 15-18 μm in diameter and having a single large acidic vacuole. The large vacuole was readily observed by phase contrast and was previously shown to stain red with acridine orange (Blanco et al. 2005). LHAs were round or ameboid in shape with a hyaline cytoplasm and were actively phagocytic. SGLs were identified as small phagocytic cells of 10–12 μm in size with a cytoplasm densely packed with granules.

LGLs aggregate immediately after the coelomic fluid is harvested by a direct cut to the body wall, unless sea water and contact with the glass surface are avoided and in addition the fluid is harvested into an ethylenediamine tetraacetic acid (EDTA)-containing solution (Blanco et al.

2008). Non-aggregated LGLs obtained by this method had acid granules that could be stained with acridine orange and appeared in a single cluster of high granularity in size vs. granularity dot plots when evaluated by flow cytometry. The cluster disappeared if sea water was added to the cell suspension, because of the massive homotypical aggregation of all LGLs (Blanco et al. 2008).

Clot formation

The clot reaction was induced through three different approaches in order to better study its haemostatic and immune aspects.

Large clot formation in a glass tube and the microscopic study of fluid obstruction

A glass tube of rectangular section was created containing four microscope slides fixed with bindings (Fig. 1a). The lower end of this tube was placed into a Petri dish filled with sea water. Coelomic fluid collected in a plastic microcentrifuge tube by a direct cut of the introvert was immediately dispensed with a pipette into the top of the glass tube and allowed to flow through into the Petri dish. When a clot was formed at the bottom of the tube in contact with sea water, the glass tube was removed from the Petri dish and observed under a microscope at low magnification and then photographed at several planes along the liquid column.

Large clot formation in plastic tube and its separation through magnetic beads

Coelomic fluid was collected from single worms via a direct cut to the body wall directly into a microcentrifuge tube containing 3×10^7 magnetic beads of 4.4 μm in diameter (Dynabeads M-450 uncoated, Dynal) in 1 ml 0.4 M NaCl and 70 μl filtered sea water. The final concentration was about 5% sea water in a final volume of 1.4 ml 0.4 M NaCl plus coelomic fluid, with slight variations attributable to small differences in worm sizes. Cells where mixed thoroughly with beads, incubated for 5 min and separated by a magnet (MPC-1, Dynal) and gentle washing with 0.4 M NaCl. The separated pellet was gently disaggregated in a remnant volume of 40 μl 0.4 M NaCl and small aliquots of about 10 μl were placed on microscope slides, observed by phase contrast microscopy and photographed.

Small clot formation induced on glass slides

Coelomic fluid was obtained from individual worms by a direct cut to the body wall and placed into a Petri dish with 4 ml 0.4 M NaCl, 5% sea water. The suspension was gently mixed by means of a pipette and 1-ml aliquots were placed on glass coverslips located inside 6-well culture plates (Nunc). In experiments in which clots were allowed to entrap foreign particles, the latter were suspended in 0.4 M NaCl and 40 μl aliquots were placed on the coverslips prior to the addition of coelomic fluid. After incubation for 15 min, the coverslips were gently washed twice in 0.4 M NaCl to separate most of the non-adherent cells and were stained supravitally or fixed for 20 min by the addition of 2 ml 2% formaldehyde in 0.4 M NaCl. The coverslips were removed from the culture plates, placed onto microscope slides, observed under both phase contrast and fluorescence microscopy and photographed. Fixed preparations were additionally processed with appropriate staining procedures as described below.

Target particles: U937 human leukemia cells, yeast cells and bacteria

U937 leukemia cells were obtained from the American Type Culture Collection (ATCC) and maintained in RPMI 1640 (Gibco) supplemented with antibiotics and 10% fetal bovine serum. Cells were suspended at 10^6/ml in 10 μM fluorescein-diacetate (FDA) in RPMI for 15 min at 37 C. The suspension was washed twice in phosphate-buffered saline (PBS) and suspended in 0.4 M NaCl just prior to being placed on coverslips for experiments. Fresh commercial yeast (*Saccharomyces cerevisiae*) was suspended at 10^8/ml in 0.4 M NaCl and incubated in 10 μM FDA for 15 min at 37 C. The suspension was washed twice by centrifugation in 0.4 M NaCl and used immediately. Bacteria (*Staphylococcus aureus*; ATCC, no. 10832) were cultured in Luria–Bertani (LB) broth at 37 C. The bacterial culture was washed twice in PBS, pH 7.0, heat-killed at 80°C for 10 min, stained with 10 μg/ml DAPI (4′,6-diamidino-2-phenylindole; Sigma, St. Louis, Mo., USA) in PBS for 30 min, washed twice in PBS by centrifugation and finally suspended at 1×10^8/ml in 0.4 M for use in experiments.

Staining of non-fixed preparations of small clots and cytoplasmic remnants with lipophilic dyes

Cell membranes, organelle membranes and lipid-rich cell remains were stained with the lipophilic dyes FM-4-64 (Molecular Probes, Invitrogen) and monodansyl cadaverine (MDC; Sigma). FM-4-64 was added at a final concentration of 40 μM from a stock solution of 16 mM in dimethyl sulphoxide (DMSO). MDC was added at a final concentration of 50 μM after the placement of 1 ml coelomic fluid on the coverslips. To recover stained cytoplasmic remnants, the cell suspension was transferred to small tubes without washing the coverslips and centrifuged at

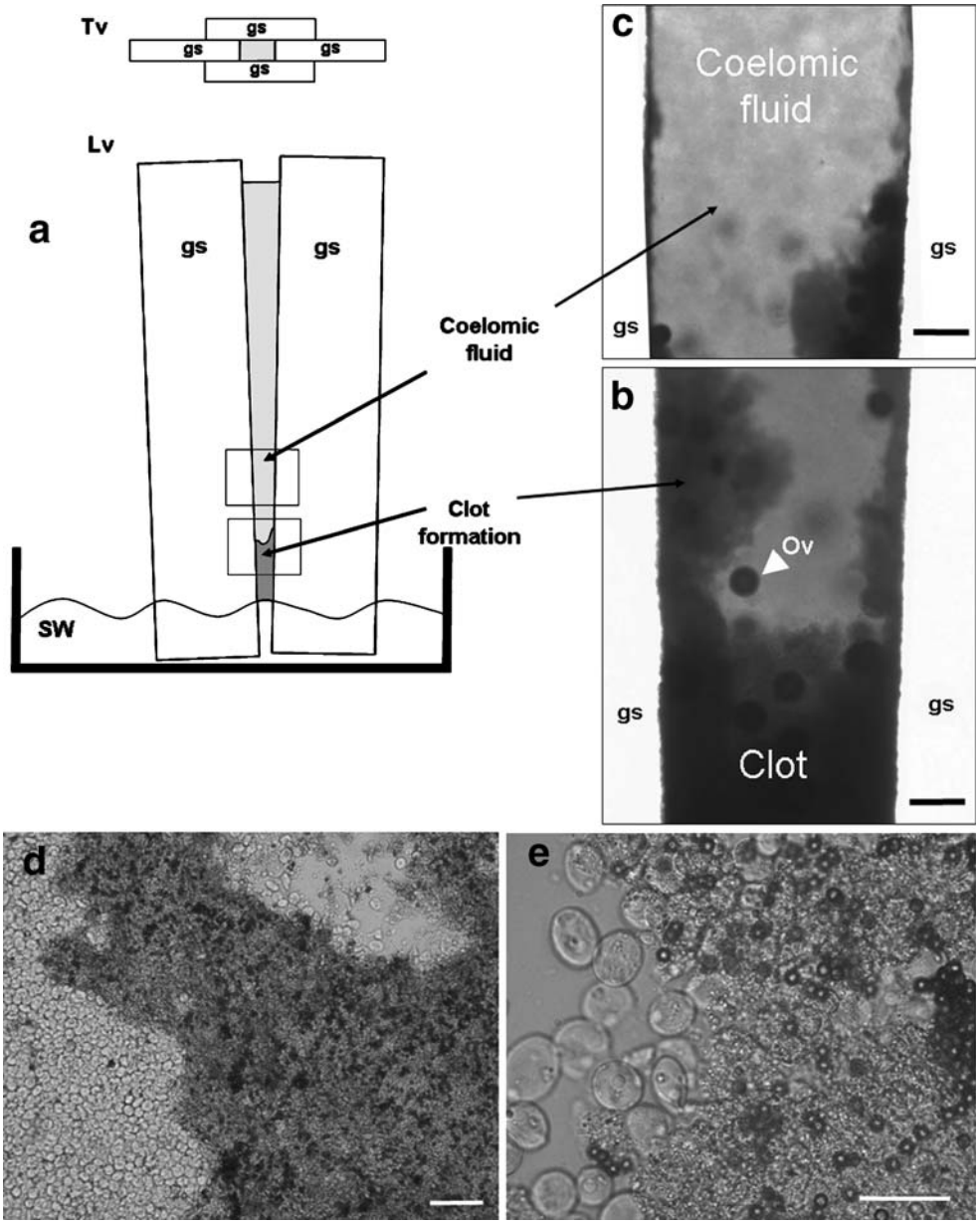

Fig. 1 Clot formation at the site of sea water (*SW*) contact (**a**–**c**) and with magnetic beads in a plastic tube (**d**, **e**). **a** Representation of the rectangular-section glass tube created with four glass slides (*gs*) as seen in a top view (*Tv*) and lateral view (*Lv*) of the glass tube. **b** Distal zone with a large clot blocking the flow. Several ovocytes (*Ov*) are seen retained by the clot, since this particular sample was from a female worm. ×40, *Bar* 200 μm. **c** Observation of the area behind the clot; non-clotting coelomocytes remain in suspension. ×40, *Bar* 200 μm. **d** Massive clotting of coelomic fluid entrapping magnetic beads. The clot was separated with a magnet and placed on a microscope slide. ×100, *Bar* 100 μm. **e** Higher magnification showing the clot edge and LGLs forming the clot by homotypic aggregation. ×400, *Bar* 30 μm

300*g* for 1 min. The supernatant was further transferred to flow cytometry tubes and analysed immediately. A second tube containing both the cell pellet and the supernatant was also run separately as a standard reference to compare the size of cell remnants with that of whole cells through forward light scatter (FSC) vs. side light scatter (SSC) dot plots.

Staining of DNA with DAPI in non-fixed preparations

Dead cells or nuclear remnants were DNA-stained by adding 5 μl of a DAPI (Sigma) stock solution (2 mg/ml) in PBS after the placement of coelomic fluid on coverslips, to yield a 10 μg/ml final DAPI concentration.

Staining live cells with FDA in non-fixed preparations

Live preparations on coverslips with entrapped DAPI-stained heat-killed bacteria were incubated with 10 μM FDA (Invitrogen) in 0.4 M NaCl for 15 min at 20°C. The suspension was washed twice in 0.4 M NaCl and the coverslips were mounted on slides and observed immediately by fluorescence microscopy.

Staining of permeabilized LGLs with sulforhodamine B in non-fixed preparations

Sulforhodamine B, a small (558 Da) water-soluble fluorescent tracer that allows the identification of permeabilized cells

(Shattil et al. 1992), was added at a final concentration of 8 μg/ml, from a 1 mg/ml stock solution in 0.4 M NaCl, to coelomic fluid placed on coverslips.

Staining of F-actin with rhodamine-phalloidin in fixed preparations

Preparations on coverslips were fixed in 4% paraformaldehyde (PFA) in NaCl 0.4 M for 30 min, washed gently twice in PBS and permeabilized in 0.5% Triton in PBS for 10 min. The preparation was washed immediately with PBS, blocked for 1 h in 1% bovine serum albumin (BSA) in PBS and stained with 1:2000 rhodamine-phalloidin (Molecular Probes, Invitrogen) in 1% BSA in PBS for 1 h. After three washes in PBS, the coverslips were mounted onto glass slides with DAPI-containing mounting fluid (Vectashield).

Staining of DNA with DAPI in fixed preparations from magnet-separated clots

Magnet-separated clots were fixed in PFA 4% in 0.4 M NaCl for 30 min, washed twice in PBS with the aid of a magnet and stained with 10 μg/ml DAPI in PBS for 30 min. The DAPI-stained pellet was gently disaggregated in a remnant volume of 40 μl 0.4 M NaCl and small aliquots of about 10 μl were placed on microscope slides, observed under fluorescence and phase contrast microscopy and photographed.

Assessment of DNA fragmentation by the TUNEL method

DNA fragmentation was evaluated by terminal deoxynucleotidyl transferase (TdT)-mediated fluorescein isothiocyanate (FITC)-2′-deoxyuridine, 5′-triphosphate (dUTP) nick-end labelling (TUNEL) by using the DeadEnd Fluorometric TUNEL System (Promega). Briefly, coverslips were fixed in 4% PFA in 0.4 M NaCl for 20 min at 4°C, washed twice in PBS, permeabilized in 0.2% Triton X-100 solution in PBS for 5 min, washed twice in PBS, incubated in 100 μl equilibration buffer (200 mM potassium cacodylate pH 6.6, 25 mM TRIS-HCl pH 6.6, 0.2 mM dithiothreitol, 0.25 mg/ml BSA, 2.5 mM cobalt chloride) and finally incubated for 1 h in equilibration buffer containing TdT and FITC-dUTP. The reaction was terminated by adding citrate buffer, after which the preparations were washed in PBS and mounted in DAPI-containing mounting fluid (Vectashield)

Negative controls were prepared by omitting TdT in the mix containing FITC-dUTP. Positive controls were prepared by incubating separate sample preparations with DNase I (10 U in buffer containing in 40 mM TRS-HCl pH 7.9, 10 mM NaCl, 6 mM $MgCl_2$, 10 mM $CaCl_2$) for 10 min, prior to nick-end labelling with TdT and FITC-dUTP.

Assessment of DNA fragmentation by agarose gel electrophoresis

Coelomic fluid was collected from single worms by cutting the body wall directly into a microcentrifuge tube containing 3×10^7 magnetic beads and 70 μl sea water. Cells where mixed thoroughly with the beads, incubated for variable time intervals between 1 min and 2 h and separated by means of a magnet as described above. The magnet-separated pellet was lysed with 500 μl lysis buffer (500 mM TRIS-HCl pH 7.5, 1 mM EDTA, 0.2% Triton X-100) and centrifuged at 13,000*g* for 10 min. The supernatant, which was assumed to contain the fragmented DNA, was precipitated overnight at -20°C in 700 μl isopropanol and 100 μl 5 M NaCl. The pellet was collected after centrifugation at 13,000*g* for 10 min, air-dried and resuspended in 10 mM TRIS-HCl, 1 mM EDTA pH 7.5. A loading buffer containing 15 mM EDTA, 2% sodium dodecyl sulphate, 50% glycerol and 0.05% bromophenol blue was added at 1:5 (v/v). Samples were electrophoresed in a 1% agarose gel and stained with 0.5 μg/ml ethidium bromide. DNA was visualized by using ultraviolet light. The DNA molecular weight marker was from PB-L Productos Bio-Logicos, UNQ, Argentina. Gel images were obtained with a digital camera (Olympus, Camedia, D-510). As a positive control for the DNA laddering pattern, we used a suspension of 5×10^6 non-clotting coelomocytes exposed to 100 mM H_2O_2 for 8 h that were further lysed and processed as described for the clot samples (Blanco et al. 2005). As a negative control for DNA degradation, we employed a suspension of 5×10^6 non-clotting coelomocytes that were lysed and processed similarly after a 1-h incubation (Blanco et al. 2005).

Light and fluorescence microscopy and flow cytometry

In all cases, the slide preparations were observed by means of an Olympus BX-51fluorescence microscope equipped with a 100-W mercury lamp, a halogen lamp for transmitted light, U-plan fluorite objectives and three fluorescence filter cubes (U-MWU2, U-MWB2 and U-MWG2 for ultraviolet, blue and green excitation light, respectively). Images were acquired with a digital Q-Color 3 Olympus camera and Image-Pro Plus 6.0 software (Media Cybernetics, USA). Image processing was performed with Image-Pro Plus 6.0. DAPI and MDC fluorescence was evaluated at an excitation wavelength of 330-385 nm (U-MWU2 filter). dUTP-FITC and FM-4-64 fluorescence was evaluated at an excitation wavelength of 450-480 nm (U-MWB2 filter). Sulforhodamine B fluorescence and rhodamine-phalloidin fluorescence was evaluated at an excitation wavelength of 510–550 nm (U-MWG2 filter). MDC and FM-4-64 fluorescence was also evaluated by flow cytometry in a Partec PAS III flow cytometer with ultraviolet 360-nm and blue 488-nm excitation

lines (100 W mercury lamp and argon laser, respectively). Events were acquired on a logarithmic scale to allow the simultaneous observation of cell remnants and intact cells in forward scatter and side scatter parameters.

Results

Large clot formation, blockade of coelomic fluid flow and entrapment of particles

Centrifugation of the coelomic fluid of sipunculans allows the separation of cells from the cell-free fluid. Although the cell-free fluid phase has never been observed to transform itself into a gel, LGLs may aggregate massively *ex vivo* in the presence of sea water, thereby forming a cellular lump or clot (Blanco et al. 2008).

In the present study, we first explored the haemostatic significance of the formation of this cellular clot in the sipunculan *Themiste petricola* by assessing its capacity to block the flow of coelomic fluid in vitro. In an attempt to simulate conditions occurring under body wall injury of the worms, whereby coelomic fluid might drain out into sea water because of positive intracoelomic pressure, we created a simple glass tube of rectangular section and a flat glass surface with a bottom edge partially immersed in sea water (Fig. 1a). When coelomic fluid collected from a worm was introduced through the top open end and allowed to flow through the tube, a small but macroscopically visible solid mass or clot was rapidly formed at the bottom end of the tube in contact with sea water (Fig. 1b). Non-clotting coelomocytes remained in suspension in those parts of the tube upstream of the site of the flow obstruction at which the clot was formed (Fig. 1c). An almost identical massive cellular clot was formed when coelomic fluid was harvested into plastic tubes in which magnetic beads had been suspended in 0.4 M NaCl/5% sea water. The cellular clot served to entrap the beads and could be separated with a magnet (Fig. 1d). Observation of the clot at higher magnification confirmed that the clot was formed by homotypically aggregated LGLs amongst which the magnetic beads had become entrapped (Fig. 1e).

Entrapment of bacteria, yeast and mammalian cells within small clots and the role of phagocytic cells

In order to explore LGL aggregation and clot formation not only with regard to its haemostatic purpose, but also as an immune response, we further induced the formation of smaller clots on glass slides and evaluated the entrapment of dissimilar foreign particles. When coelomic fluid was dispensed onto glass slides containing suspensions of fluorescent bacteria, several small round clots were found to entrap them (Fig. 2a, b). Fluorescent bacteria were also observed elsewhere away from the clot, having been phagocytosed by two non-clotting coelomocyte cell types: SGLs and LHAs (Fig. 2c, d).

In addition, SGLs but not LHAs where observed located at the edges of the clots with phagocytosed bacteria (Fig. 2e, f). A similar approach revealed fluorescent yeast and fluorescent human U937 leukemia cells entrapped in small clots (Fig. 2g–j), thus underscoring the broad specificity of particles that could be captured by this mechanism.

Process of cell death in association with entrapment of foreign particles

The clot is initiated by live LGLs that are activated and aggregate but rapidly die leaving their remains to become a key structural component of the clot. Thus, we first evaluated changes in nuclear morphology within the small clots by staining magnet-separated fixed preparations with DAPI. Nuclei at central areas were pale, small and irregularly shaped indicating low DNA content as opposed to brighter, round and larger nuclei at the peripheral zones of the clot (Fig. 3a, b). In addition, nuclei having condensed and fragmented chromatin were often seen at the peripheral areas of the clot (Fig. 3c). The staining of live preparations with FDA, an indicator of metabolic activity in live cells, confirmed that the central areas of the clots in which entrapped bacteria were identified became rapidly non-viable, whereas peripheral zones conserved viability (Fig. 3d). Moreover, the permeation of cells forming the clot, but not of cells elsewhere away from the clot, was evidenced by staining with sulforhodamine B, whereas no extracellular protein fibres appeared to be stained by this fluorescent probe (Fig. 3g, h). DNA degradation within the clot was further evidenced by agarose gel electrophoresis of fragmented DNA obtained from magnet-separated clots. A smeared pattern of mono-nucleosome-size DNA fragments, but not a laddering pattern, was consistently observed as early as 15 min and up to 60 min after clot formation indicating a massive and rapid degradation of DNA within the clot (Fig. 4). Thus, although some nuclei were observed to have condensed and fragmented chromatin, the absence of a DNA laddering pattern was interpreted as a strong indicator that cell death was not attributable to apoptosis (Kroemer et al. 2009).

Phagocytosis, by SGLs and LHAs, of cytoplasmic and nuclear remnants shed from clots

Although our observations suggested that cell death preferentially occurred first at central areas and progressed

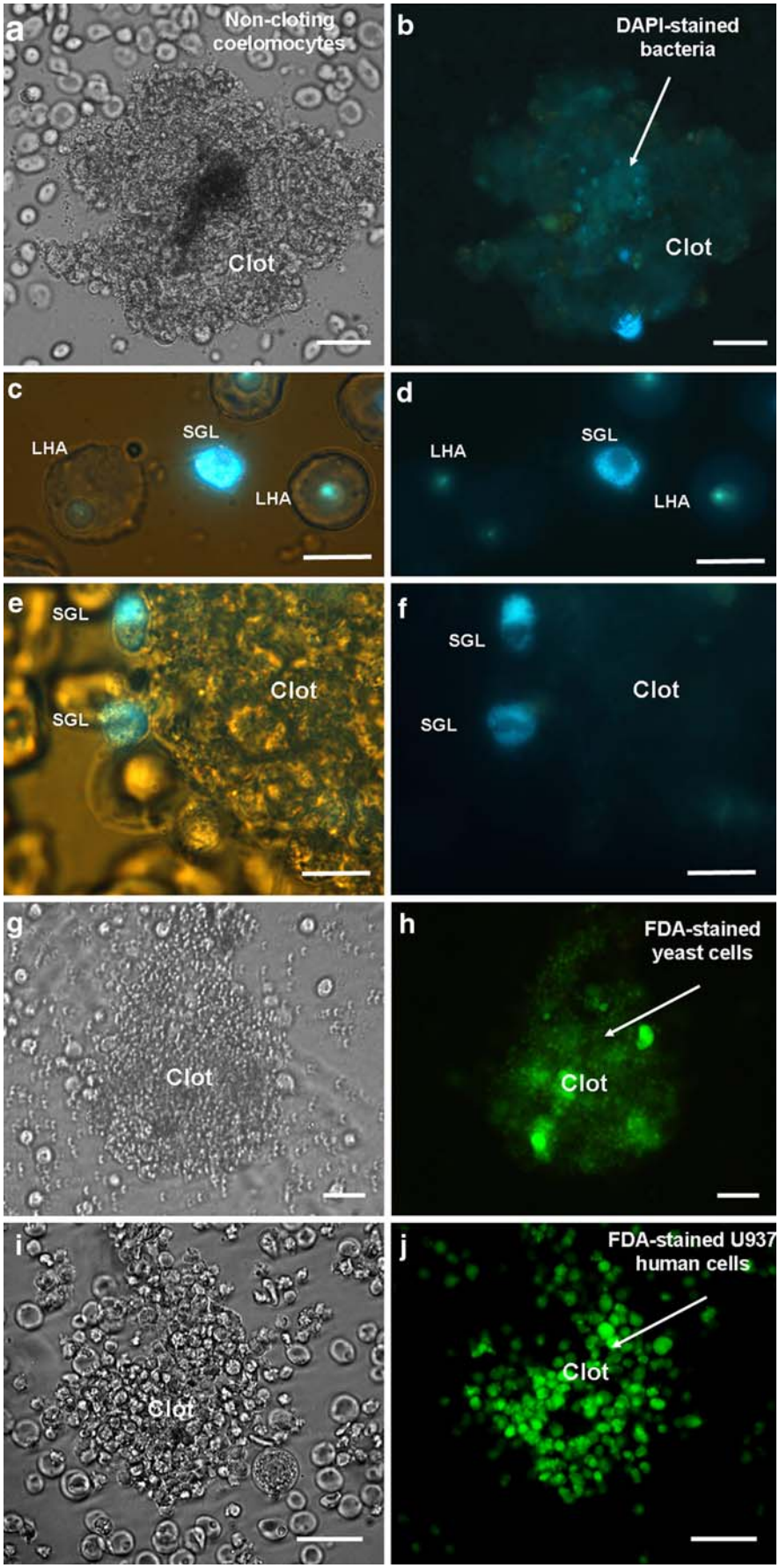

Fig. 2 Entrapment of bacteria, yeast and human cells in small clots and phagocytosis by small granular leukocytes (*SGL*) and large hyaline amebocytes (*LHA*). **a** Phase contrast image of a clot formed over a suspension of DAPI-stained heat-killed bacteria. The clot was spheroid in shape and thus several images could be obtained at various focal planes. In contrast, non-clotting coelomocytes lying away from the clot remained at a single focal plane. ×100, *Bar* 50 μm. **b** *Blue* fluorescent DAPI-stained bacteria were entrapped within the clot (same field as that shown in **a**). **c** Combined fluorescent and phase contrast image of SGLs and LHAs located away from the clot and showing phagocytosed DAPI-stained bacteria within the cytoplasm. ×1000, *Bar* 15 μm. **d** Fluorescent image of the same field as that shown in **c**. Bacteria were found within a densely packed cytoplasm in SGLs, but with a more restricted cytoplasmic distribution in LHAs, often occurring within the characteristic large vacuole of these cells. **e** Combined phase contrast and fluorescent image of bacteria phagocytosed by SGLs observed at the edge of a small clot. A small number of SGLs were frequently observed at the margin. ×1000, *Bar* 15 μm. **f** Fluorescent image of the same field as that in **e**. **g** Phase contrast image of yeast cells entrapped by a small clot. ×100, *Bar* 50 μm. **h** Fluorescent image of the field shown in **g** showing *green* fluorescent fluorescein-diacetate (FDA)-stained yeast cells entrapped within the clot. **i** Phase contrast image of a small clot formed over a suspension of non-clustering human U937 cells. ×100, *Bar* 50 μm. **j** Fluorescent image of the field in **i** showing *green* fluorescent FDA-stained live U937 human cells entrapped by a small clot

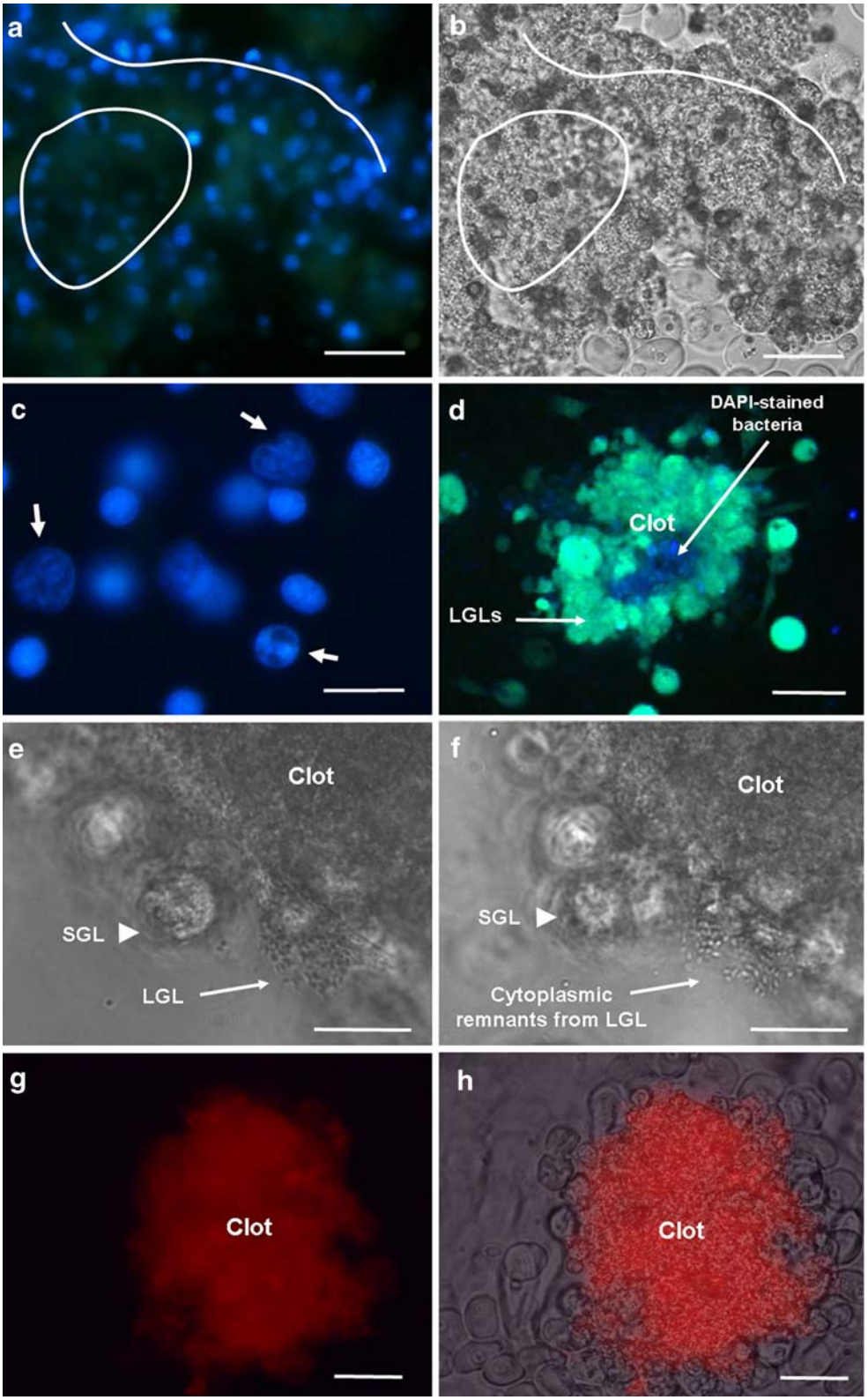

Fig. 3 Indicators of cell death in homotypically aggregated LGLs forming the clot with evidence of nuclear and cytoplasmic breakdown. **a** Fluorescence image of a magnet-separated fixed preparation stained with DAPI showing a small clot entrapping magnetic beads. The central areas of the clot showed poor staining of nuclei indicating extensive DNA degradation (*encircled area*). In contrast, nuclei at the peripheral zones of the clot (*curved line*) were better stained indicating that the DNA was degraded to a lower extent than that in cells located more deeply within the clot. ×200, *Bar* 30 μm. **b** Phase contrast image of the preparation shown in **a** giving a clearer view of peripheral and central areas of the clot. **c** Fluorescence image of DAPI-stained nuclei observed at the peripheral zones of the clot, showing chromatin condensation, fragmentation and nuclear membrane ripples (*arrow*). ×1000, *Bar* 10 μm. **d** A small clot entrapping DAPI-stained bacteria. Unfixed preparation stained with the supravital dye FDA. *Green* fluorescence at the periphery of the clot indicated that homotypically aggregated LGLs were viable, while the absence of green fluorescence at the central area of the clot indicated a loss of cell viability at that site. ×200, *Bar* 30 μm. **e**, **f** Two successive phase contrast images showing disintegration of a LGL located at the edge of clot (*arrow* in **e**) and shedding of the cytoplasmic remnants into the clot neighbourhood (*arrow* in **f**). An SGL is present in both images crawling around the edge of the clot (*arrowhead*). ×1000, *Bar* 15 μm. **g** A small clot stained with sulforhodamine B, a dye that stains intracellular proteins in permeabilized cells. ×200, *Bar* 30 μm. **h** Overlaid phase contrast and fluorescence image of the same field shown in **g** showing that only LGLs at the clot were stained by sulforhodamine B

to the periphery, the shedding of small cytoplasmic and nuclear remnants into the clot neighbourhood was also observed in some preparations (Fig. 3e, f). To explore the fate of these cytoplasmic remnants shed from the clot, we stained live preparations induced on glass slides with the lipophylic dye FM-4-64. This dye not only stains cell membrane but is further routed through the endocytic pathway of the cells and stains endosomes, phagocytic

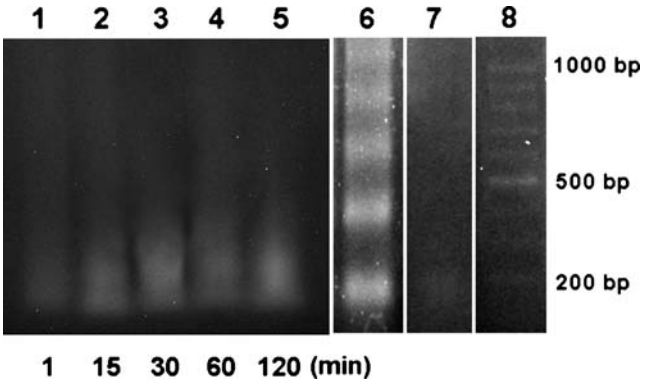

Fig. 4 Time course evaluation of DNA degradation within a magnet-separated clot. Electrophoresis of DNA in 1% agarose gel. *Lanes 1–5* DNA extracted from cells recovered from magnet-separated clot masses at increasing time points (*min*) after clot formation. *Lane 6* DNA laddering pattern (positive control) as observed in non-clotting apoptotic coelomocytes (mainly haemerythrocytes and LHAs) obtained after 8 h exposure to H_2O_2). *Lane 7* DNA from non-clotting coelomocytes not exposed to H_2O_2 (negative control). *Lane 8* Molecular weight marker

vacuoles, many organelles and even the nuclear membrane (Vida and Emr 1995). Strong diffuse fluorescence originating from several focal planes of the multicellular spheroid of aggregated LGLs was observed at the clots (Fig. 5a, b). In contrast, non-clotting cells lying away from the clots remained at a single focal plane and were clearly stained at their cell membranes and phagocytic vacuoles (Fig. 5c). Most importantly, this dye allowed us to stain small cytoplasmic remnants shed from the clot and to observe clearly the phagocytosis of these remnants by LHAs and SGLs (Fig. 5d, e). As occurred with preparations exposed to bacteria, the cytoplasm of SGLs was densely packed with endocytosed membranes, whereas lower amounts of such membranes were observed in LHAs (Fig. 5e).

Next, we recovered cytoplasmic remnants from supernatants of clots previously stained with either FM-4-64 or MDC, another fluorescent lipohilic dye (Munafo and Colombo 2001; Pincus et al. 1975), and studied these supernatants by flow cytometry in order to identify and quantify the presence of small cytoplasmic remnants stained by either red (FM-4-64) or blue (MDC) fluorescence (Fig. 6). These fluorescent membrane remnants appeared, in FSC and SSC, as a single cluster that was smaller than that of whole cells (Fig 6c, d), thus confirming the results from fluorescence microscopy.

To obtain definitive evidence of the phagocytosis of cytoplasmic remnants by SGLs and LHAs, we concentrated a preparation of MDC-stained remnants from one worm and placed this on a glass slide. Then, a new clot was allowed to form with coelomic fluid from a second worm. As expected, MDC-stained cytoplasmic remnants were found in SGLs and LHAs and entrapped within the clot (Fig. 5f–h)

Dissimilar cytoskeletal changes in LGLs and SGLs

To obtain further evidences of the differential and perhaps complementary roles of LGLs and SGLs during clot formation and particle entrapment, we evaluated the pattern of cytoskeletal changes by staining preparations of glass-adhered cells with the F-actin marker phalloidin. The most striking arrangements occurred in LGLs. These cells spread extensively in all directions and fused to each other to form small clots (Fig. 7a–c). In addition, these small clots formed a large veil-like structure composed of F-actin-rich cytoskeletal components that spread well beyond the apparent edge of the clot, as compared with phase contrast images (Fig. 7c, g, h). In contrast, SGLs often showed a polarized pattern similar to that of migrating cells (Mitchison and Cramer 1996; Stossel 1993) with leading F-actin-rich edges (lamellipodia) and trailing edges with a low F-actin content (uropodia; Fig. 7d, e).

When preparations to be stained with phalloidin-rhodamine were made by decanting coelomic fluid over suspensions of DAPI-stained bacteria, SGLs showed internalized blue fluorescent bacteria; this confirmed that these phagocytic cells corresponded to the polarized cells with lamellipodia and uropodia. In addition, SGLs were sometimes observed with a non-polarized cytoskeletal arrangement with thick filopodia extending in all directions and in contact with external bacteria, thus indicating active phagocytosis by these cells at specific locations rather than migration (Fig. 7f-f'''). Limited numbers of free DAPI-stained bacteria were observed immersed in the veil-like structure that emerged from the clot suggesting it might have a role aiding phagocytosis (Fig. 7g, h).

Nuclear remnants had fragmented DNA and were phagocytosed by SGLs and LHAs

Having demonstrated that cytoplasmic remnants were shed from the clot and phagocytosed by SGLs and LHAs, we next turned to explore the fate of nuclear remnants. As noted above, extensive DNA degradation was observed within the clot but, since some LGLs were observed to disintegrate their cytoplasm into small particles, the nuclear remnants containing fragmented DNA might also have been shed from the clot and further scavenged by SGLs and LHAs. To identify nuclear remnants with partially degraded DNA, we used non-fixed small clot preparations in which DAPI was present during clot formation as a supravital DNA dye, on glass slides. Our purpose was to stain with DAPI those nuclear fragments originating from dead LGLs while leaving viable cells unstained because DAPI only stains cells with a permeable cell membrane (Shapiro 2003). As expected, blue fluorescent DAPI-stained nuclear remnants where found in the cytoplasm of LHAs and

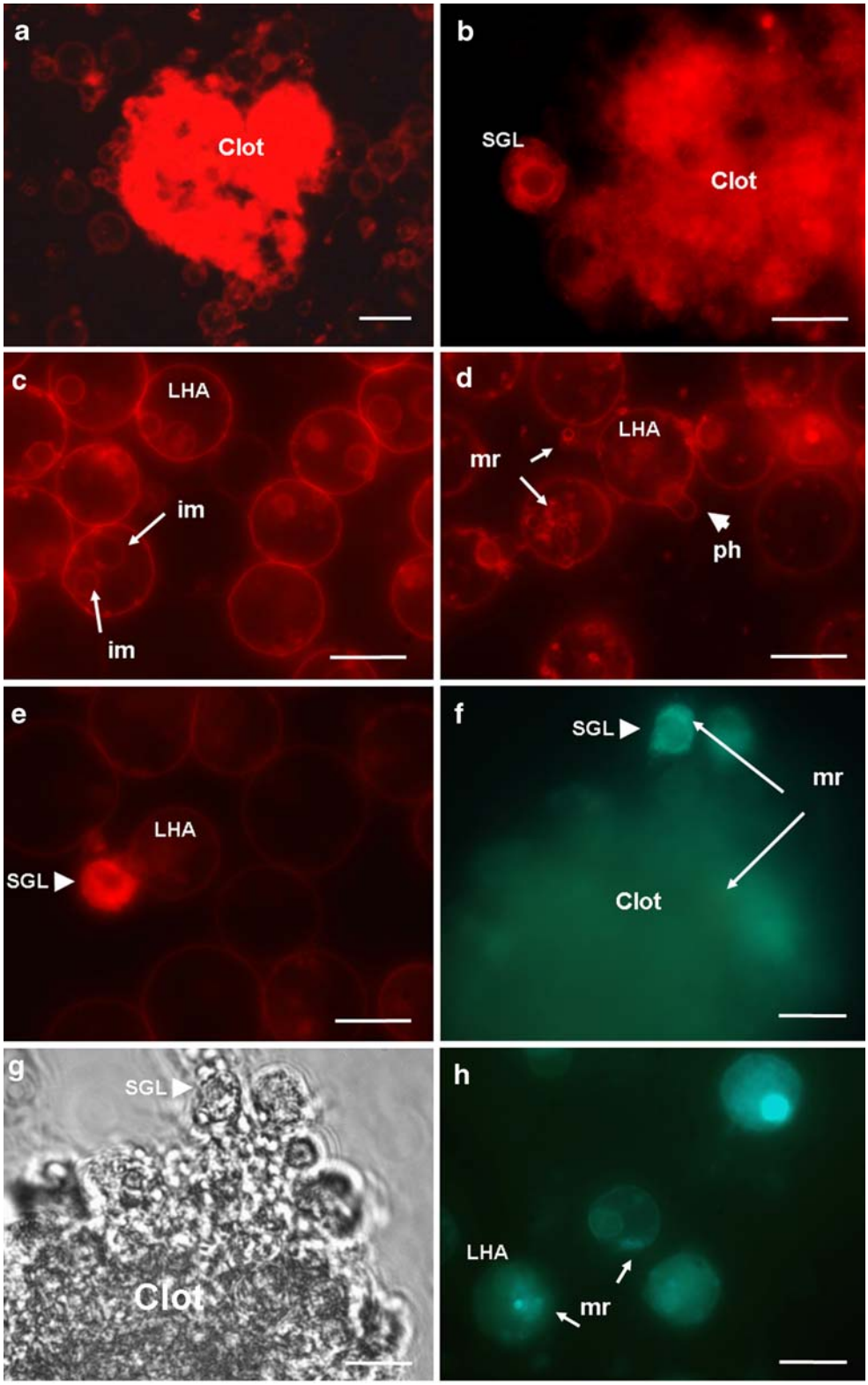

SGLs indicating that these remnants were being shed from the clot and scavenged by these cells (Fig. 8a).

To confirm these findings and to determine whether these nuclear remnants corresponded to fragmented DNA, we evaluated fixed preparations of small clots formed in glass surface with the nick-end DNA-labelling technique (TUNEL). Fragmented DNA was largely detected in the cytoplasm of SGLs and also within the clots, albeit to a

◀ **Fig. 5** Phagocytosis of cytoplasmic remnants stained with lipophylic dyes FM-4-64 and monodansyl cadaverine (MDC). **a** Live preparation stained with FM-4-64 and showing a small clot formed on the glass surface. The dense cloudy fluorescence arising from several focal planes indicated that the clot contained large amounts of LGL-derived lipid membranes. In contrast, non-clotting cells remained in a single focal plane and where stained at the cell membrane and at internal membranes of the endosomic route. ×200, *Bar* 30 μm. **b** Clot staining did not allow the distinction of cell contours or internal structures of aggregated LGLs. An SGL with clear definition of the cell membrane, nuclear membrane and cytoplasmic content can be seen at the clot edge. ×1000, *Bar* 15 μm. **c** LHA lying away from the clot showing staining of the cell membrane and internal membranes (*im*) outlining the characteristic large vacuole of these cells and the nuclear membrane. ×1000, *Bar* 15 μm. **d** Small membrane remnants (*mr*) observed lying free between cells, but being actively phagocytosed (*ph*) by LHAs and within LHAs at several locations within the cytoplasm. ×1000, *Bar* 15 μm. **e** SGL observed lying away from the clot with its cytoplasm densely packed with membrane remnants. ×1000, *Bar* 15 μm. **f** Membrane remnants (stained with the lipophylic dye MDC) obtained from the coelomic fluid of one worm and entrapped in small clots by the coelomic fluid of a second worm, as indicated by *blue* fluorescence of the clot. *Blue* fluorescence within SGLs of the second worm demonstrated phagocytosis of MDC-stained membrane remnants (*mr*) from the first worm. ×1000, *Bar* 15 μm. **g** Phase contrast image of the same preparation as that shown in **f**. **h** *Blue* fluorescence within LHAs of the second worm lying away from the clot and showing phagocytosis of MDC-stained membrane remnants (*mr*) from the first worm. ×1000, *Bar* 15 μm

much lower extent (Fig. 8b–d). Positive controls of the DNase-I-treated preparations confirmed that green fluorescence corresponded to fragmented DNA nick-end labelling (Fig. 8e, f). Negative controls with no TdT enzyme showed no green fluorescence and confirmed the specificity of TUNEL (data not shown).

Discussion

Clot formation in sipunculans is both a straightforward haemostatic function and a first-line immune response. In this study, we have evaluated some aspects of the interplay between cells directly involved in clot formation and cells having the complementary role of phagocytosing self products, such as cytoplasmic and nuclear remnants shed from the clot, and non-self material. The combination of immune and haemostatic functions has created some historical controversies about whether clotting is present in sipunculans and whether sipunculans form nodules and capsules as occurs in insects and crustaceans (Cushing and Boraker 1975; Dybas 1976; Rice 1993; Towle 1975; Triplett et al. 1958). A simple gadget designed to create a liquid column opened at the bottom end in contact with sea

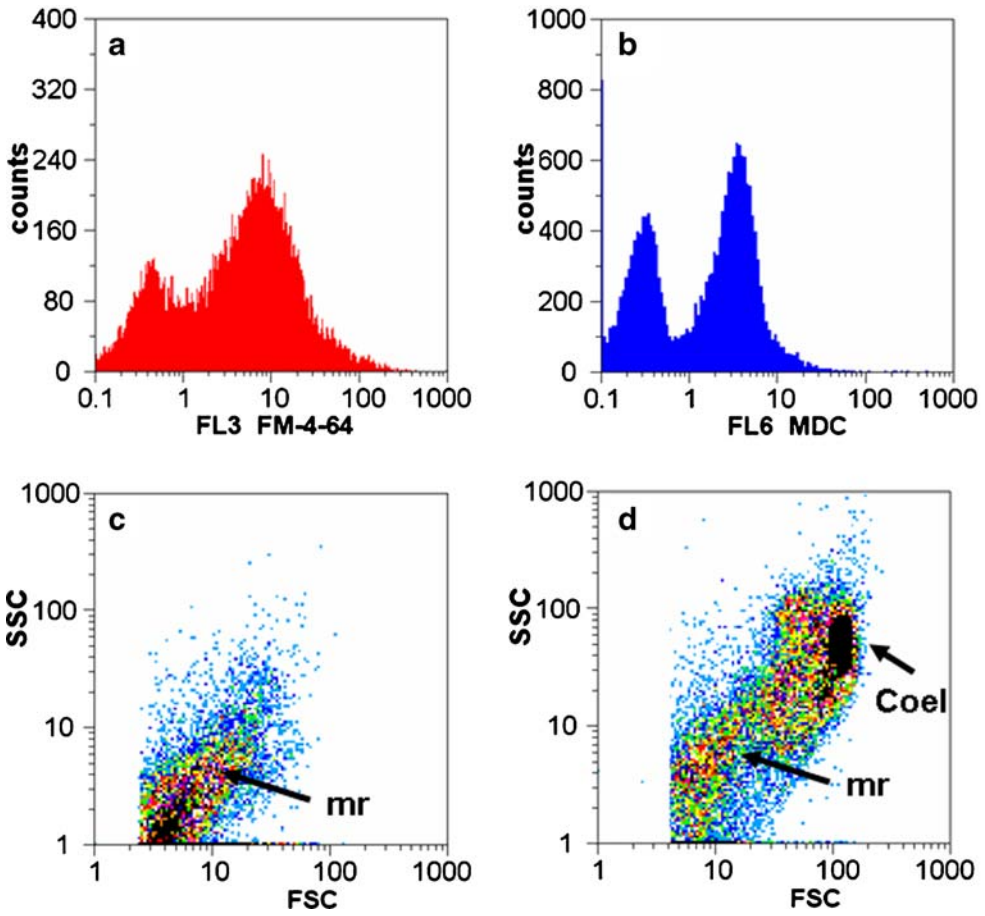

Fig. 6 Flow cytometry of membrane remnants isolated from clot supernatant stained with lipophylic dyes FM-4-64 or MDC. **a** *Red* fluorescence of membrane remnants detected in supernatants of preparations stained with FM-4-64. **b** *Blue* fluorescence of membrane remnants detected in supernatants of preparations stained with MDC. **c** Forward (*FSC*) vs. side (*SSC*) light scatter plot of membrane remnants (*mr*) detected in supernatants of preparations. **d** Forward (*FSC*) vs. side (*SSC*) light scatter plot of a suspension containing both membrane remnants (*mr*) and coelomocytes (*Coel*) showing the relative size of remnants to coelomocytes

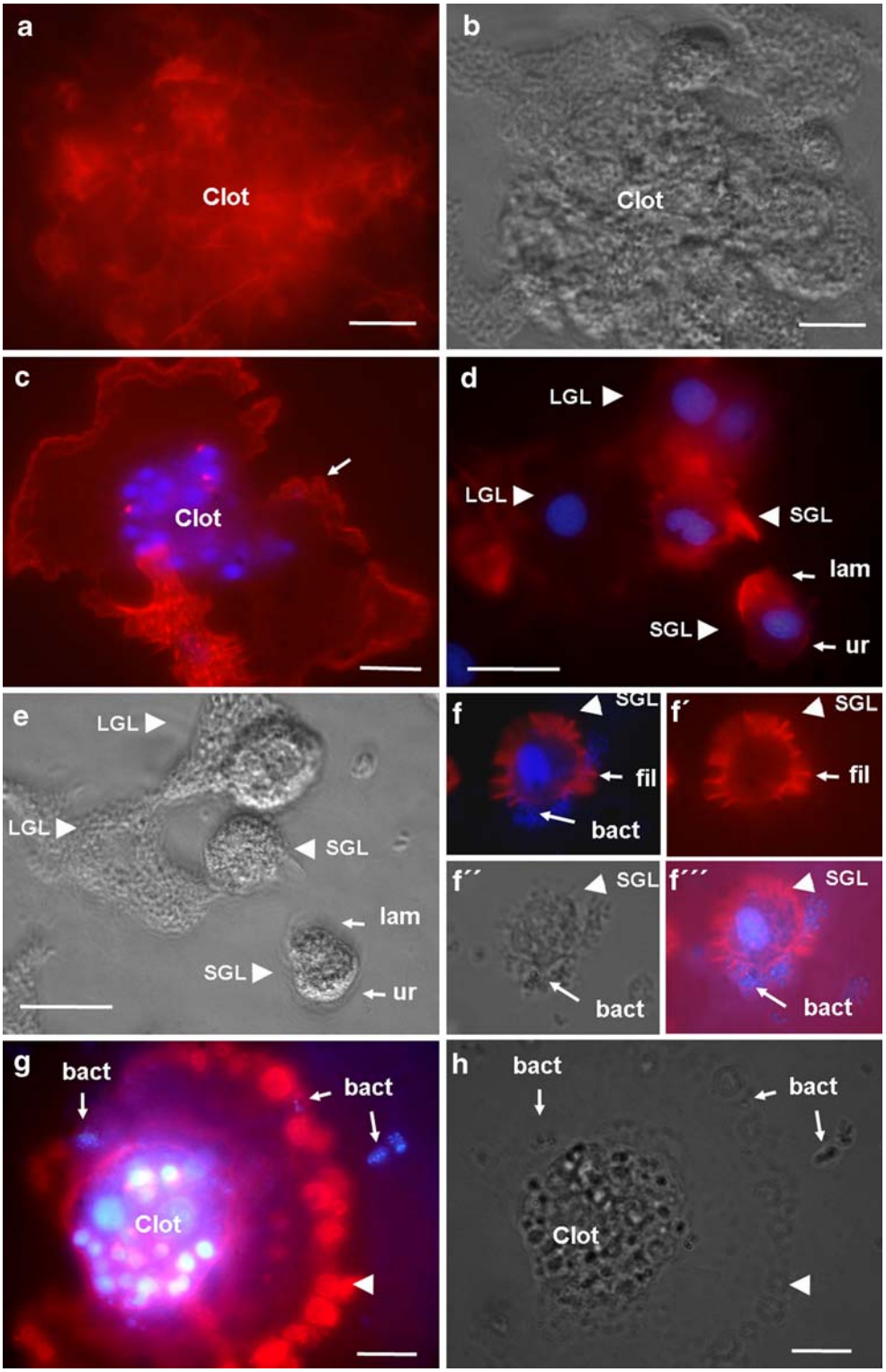

Fig. 7 Cytoskeletal arrangement of LGLs and SGLs during clot formation. **a** Phalloidin-rhodamine staining of F-actin in a clot formed after glass contact. Aggregated LGLs formed a syncytial mass in which the cytoskeletal arrangement of the clot itself appeared as a uniform mesh of F-actin fibres. **b** Phase contrast image of the preparation shown in **a**. **c** A small clot stained with phalloidin-rhodamine and counterstained with DAPI showing the extensive spread in all directions away from the clot, with F-actin-rich zones at the clot margins (*arrow*). **d** LGLs spreading in several directions and an SGL with a polarized cytoskeletal arrangement of F-actin characteristic of migrating cells with lamellipodia (*lam*) at the leading edge and uropodia (*ur*) at the trailing edge. The cell boundaries of SGLs could be easily recognized but not that of LGLs because most of these cells appeared fused to each other. **e** Phase contrast image of the preparation in **d** showing the cell boundaries of LGLs and SGLs more clearly. **f–f‴** Cytoskeletal arrangement of an SGL phagocytosing some DAPI-stained bacteria. Thick filopodia (*fil*) formation appeared to participate in the phagocytosis of the bacteria. **f** Phalloidin-rhodamine counterstained with DAPI. **f′** Phalloidin-rhodamine. **f″** Phase contrast. **f‴** Phalloidin-rhodamine, DAPI and phase contrast. **g** DAPI-stained bacteria (*bact*) were occasionally found entrapped in the veil-like structure surrounding the clot core. This veil-like structure appeared as an integral part of the cytoskeletal arrangement of the clot with F-actin-rich zones at the edges (*arrowhead*). **h** Phase contrast image of the preparation in **g** showing that the veil-like structure with F-actin-rich margins (*arrowhead*) extended well beyond the apparent edge of the clot. ×1000, *Bars* 15 μm

water had allowed us to demonstrate that a gross cellular clot occurs at the opened end and prevents the drainage of coelomic fluid from higher in the fluid column. Our finding that this large and massive clot prevents fluid flow under low hydrostatic pressure highlights its haemostatic role and indicates that it might serve to create a rapid seal to prevent the loss of fluid upon body wall injury. Thus, effective haemostasis occurs in this marine worm even though cell-free coelomic fluid does not congeal. LGLs are not trapped in a gel mesh but constitute the structure of the clot

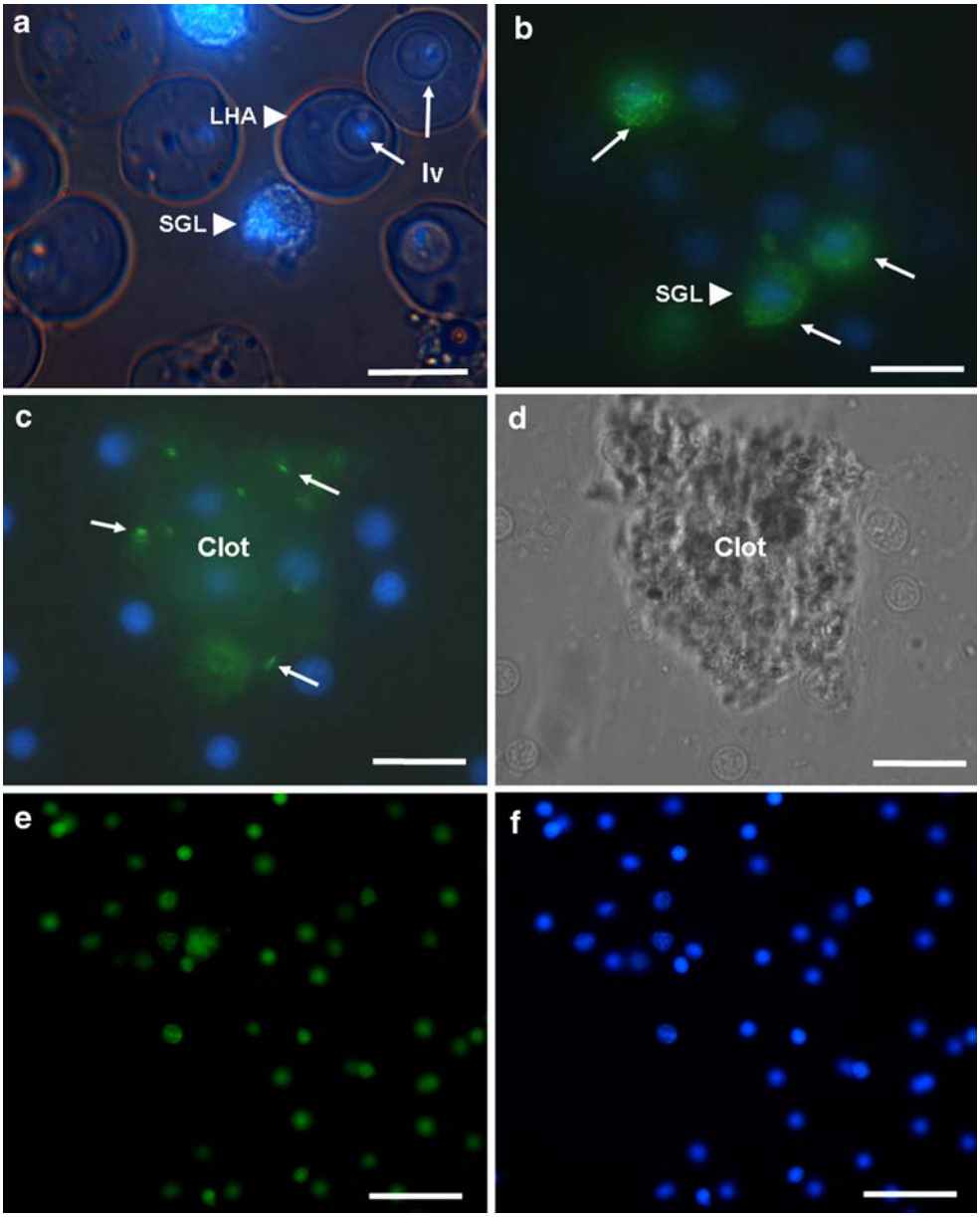

Fig. 8 Phagocytosis of DNA-containing nuclear fragments by SGLs and LHAs. **a** Combined phase contrast and fluorescent image of a live preparation in which DAPI was present as a supravital stain during clot formation allowing the staining of dead cells and DNA-containing nuclear remnants. DAPI-stained nuclear remnants were taken up by SGLs and were seen throughout the cytoplasm with the exclusion of the nucleus indicating SGLs remained viable. LHAs also phagocytosed nuclear remnants and were observed within the large vacuole (*lv*). ×1000, *Bar* 15 μm. **b** TUNEL staining of a small clot. Significant amounts of fragmented DNA observed within the cytoplasm of SGLs (*arrows*) were located at the boundaries of a small clot. ×1000, *Bar* 15 μm. **c** TUNEL staining of a small clot with scanty amounts of fragmented DNA (*arrows*) indicating it was being either rapidly degraded within the clot or taken up by SGLs. ×1000, *Bar* 15 μm. **d** Phase contrast image of the preparation in **c** illustrating that the location of TUNEL-positive fragmented DNA corresponded to that of the clot. **e** DNase-I-treated preparation showing TUNEL-positive *green* fluorescence in nuclei of all clotting and non-clotting cells. ×400, *Bar* 30 μm. **f** Same preparation as in **e** illustrating that DAPI-staining of all nuclei corresponded to the same cells with positive TUNEL fluorescence. ×400, *Bar* 30 μm

itself. The site of sea water contact appears to dictate the point at which LGL aggregation forms the clot. This finding introduces a model of haemostasis different from current arthropod and vertebrate models and challenges the well-established paradigm that blood or haemolymph coagulation is attributable to the clotting of plasma rather than to changes in the cellular constituents. We have also observed that extensive clots can form on the exposure of coelomic fluid to magnetic beads in small tubes and that the clot can be separated from the tube with a magnet. Since particles are entrapped in the clot, the result highlights that, in addition to sea water, foreign material contact also contributes to the definition as to where clotting will take place and underscores the immune significance of massive clotting. In contrast, small round clots form around bacteria placed in suspension on glass coverslips. These small cellular clots are to some extent morphologically reminiscent of the nodules described in insects (Gandhe et al. 2007; Lavine and Strand 2002; Ratcliffe and Gagen 1977). The homotypic aggregation of LGLs that form the clot acts as a mesh in which potential pathogens can be captured. Entrapment of particles is almost immediate and appears to be of broad specificity, since magnetic beads, bacteria, yeast or even mammalian cells can be entrapped in clots.

The fate of LGLs after aggregation and activation is cell death, which appears to occur first at central areas of the clot, whereas LGLs at peripheral zones seem to remain viable for a slightly longer time as judged by the observation of metabolic activity. However, features such

as nuclei with condensed and fragmented chromatin and the shedding of cytoplasmic and nuclear remnants from dead LGLs have also been observed at the peripheral areas of the clot. In addition, bead-separated clots show only mono-nucleosome-size DNA at all time points evaluated, with no DNA laddering pattern, again indicating that DNA is being degraded rapidly. Our previous studies have shown that LGL acid granules are disintegrated at central areas of the clot, as assessed by supravital staining with acridine orange (Blanco et al. 2008). Thus, the clot aids to entrap, immobilize and destroy microbes, even with the sacrifice of self cells, providing a degradative environment within the clot in which extensive self and potentially foreign DNA destruction takes place. Of note, recent studies have demonstrated a strong modulation of immune response of insects by extracellular nucleic acids (Altincicek et al. 2008). Apoptosis and programmed cell death are no longer considered synonyms and the absence of apoptosis does not rule out the occurrence of non-apoptotic forms of programmed cell death (Kroemer et al. 2009). Necrosis may be an accidental uncontrolled form of cell death or may be finely regulated by a set of signal transduction pathways and catabolic mechanisms, although it is still largely identified in negative terms by the absence of apoptotic or autophagic markers (Kroemer et al. 2009). Our morphological evaluation argues in favour of necrosis occurring under regulated conditions. The morphological features of necrosis within the clot seem not to occur accidentally or in an uncontrolled form but are regulated to proceed strongly within the central areas, with DNA degradation and lysosomal rupture, and more gently or perhaps in a delayed manner at the clot edges. The finding that LGLs, but not cells lying away from the clot, become permeable to the water-soluble small 558-Da tracer sulforhodamine B, which binds to proteins and exhibits red fluorescence (Shattil et al. 1992), strongly suggests that the permeation and massive influx of other molecules, such as extracellular Ca^{2+}, have an important role in the rapid occurrence of LGL death. In addition, staining with sulforhodamine B has revealed no extracellular matrix of clot fibres composed of coagulated proteins, as is observed in arthropod clots in which such fibres can be stained together with entrapped haemocytes (Bidla et al. 2005; Scherfer et al. 2004).

Unlike aggregated LGLs, LHAs and SGLs remain viable in all preparations and exhibit a scavenging role, phagocytosing cytoplasmic and nuclear remnants of LGLs and bacteria. SGLs in particular appear to wonder in close contact with the edges of the clot and in locations away from the clot. In contrast, LHAs have not been seen in close proximity to the clot but only elsewhere, thus fulfilling a more clot-distant ancillary phagocytic role. Surprisingly, the assessment of the cytoskeletal arrangement of cells involved in clot formation via the F-actin polimerization pattern has shown a veil-like thin structure extending from the clots. This arrangement might have some role in facilitating the immobilization of particles and phagocytosis by SGLs. The latter cells, as opposed to LGLs, have a high F-actin content with a pattern compatible with polarized migrating cells, sometimes with multiple filopodia aiding the phagocytosis of bacteria. In our previous studies, assessment by Giemsa staining has been strongly suggestive of phagocytosis of nuclear and cytoplasmic remnants by non-dying cells (Blanco et al. 2008). However, morphological similarities between early activated LGLs and SGL have not allowed us to ascertain the dissimilar role of the latter. Here, we have clearly identified SGL as a different cell type actively involved in scavenging cytoplasmic and nuclear remnants in close proximity to the clot. By several staining approaches, we have confirmed that SGLs are closely connected to, but not part of, the clot itself. Indeed, these cells appear to wonder around the clot and, if found in central areas of the clot, are located at the top or bottom focal planes of the spheroid-shaped clots. The cytoskeletal arrangement of SGLs often correspond either to that of polarized migrating cells with lamellipodia and uropodia or to phagocytosing cells with thick filopodia in contact with bacteria. In contrast, the cytoskeletal arrangement of LGLs in small clots corresponds to that of non-migrating cells that extensively spread in all directions and fuse to each other. The F-actin-rich cytoskeletal structures are only focal contacts made on the glass surface. Staining supravitally with DAPI has shown a paradoxical image of SGLs with a clear nucleus and stained cytoplasm indicating the phagocytosis of DAPI-stained LGL nuclear remnants. The nick-end labeling method has also shown a paradoxical staining of SGLs with a clear nucleus and stained cytoplasm indicating the presence of fragmented DNA as a result of phagocytosis. Similarly, cytoplasmic remnants obtained from the clot supernatant and previously stained with lipid dye MDC are uptaken by SGLs and show intense staining of the cytoplasm. Thus, we conclude SGLs have a central role in scavenging nuclear and cytoplasmic remnants of dead and disintegrated LGLs shed from the clot and microbes or particles partially immobilized at the clot periphery or free elsewhere other than the clot. Thus, clot formation might contribute to the congregation of cellular immune effectors at the site of pathogen entrance and entrapment, as has recently been highlighted by Haine et al. (2007) who have reviewed the functional consequences of clotting in insects. Our findings support the idea of the presence of a common haemostatic-immune strategy adopted by sipunculans, where clotting cells and non-clotting phagocytic cells have complementary roles as first- and second-line defenses, respectively, in the response to the intrusion of pathogens within an integrated system.

References

Altincicek B, Stotzel S, Wygrecka M, Preissner KT, Vilcinskas A (2008) Host-derived extracellular nucleic acids enhance innate immune responses, induce coagulation, and prolong survival upon infection in insects. J Immunol 181:2705–2712

Bidla G, Lindgren M, Theopold U, Dushay MS (2005) Hemolymph coagulation and phenoloxidase in *Drosophila* larvae. Dev Comp Immunol 29:669–679

Blanco GA (2007) Involvement of apoptosis-like cell death in coelomocytes of *Themiste petricola* (Sipuncula) in the formation of a cellular clot with haemostatic and immune functions. In: Valentino RG (ed) New cell apoptosis research. Nova Biomedical Books, New York, pp 121–160

Blanco GA, Alvarez E, Amor A, Hajos S (1995) Phagocytosis of yeast by coelomocytes of the sipunculan worm *Themiste petricola*: opsonization by plasma components. J Invertebr Pathol 66:39–45

Blanco GA, Bustamante J, Garcia M, Hajos SE (2005) Hydrogen peroxide induces apoptotic-like cell death in coelomocytes of *Themiste petricola* (Sipuncula). Biol Bull 209:168–183

Blanco GA, Malchiodi EL, De Marzi MC (2008) Cellular clot formation in a worm: entrapment of foreign particles, cell death and identification of a PGRP-related protein. J Invertebr Pathol 99:156–165

Bohn H (1986) Hemolymph clotting in insects. In: Brehelin M (ed) Cells, molecules, and defense reactions. Springer, Berlin, pp 188–207

Cushing JE, Boraker DK (1975) Some specific aspects of cell-surface recognition by sipunculid coelomocytes. Adv Exp Med Biol 64:35–44

Doyle D (2006) William Hewson (1739-74): the father of haematology. Br J Haematol 133:375–381

Dunn CW, Hejnol A, Matus DQ, Pang K, Browne WE, Smith SA, Seaver E, Rouse GW, Obst M, Edgecombe GD, Sorensen MV, Haddock SH, Schmidt-Rhaesa A, Okusu A, Kristensen RM, Wheeler WC, Martindale MQ, Giribet G (2008) Broad phylogenomic sampling improves resolution of the animal tree of life. Nature 452:745–749

Dybas L (1976) A light and electron microscopic study of the ciliated urn of *Phasolosoma agassizii* (Sipunculida). Cell Tissue Res 169:67–75

Gandhe AS, John SH, Nagaraju J (2007) Noduler, a novel immune up-regulated protein mediates nodulation response in insects. J Immunol 179:6943–6951

Gregoire C (1951) Blood coagulation in arthropods. II. Phase contrast microscopic observations on hemolymph coagulation in sixty-one species of insects. Blood 6:1173–1198

Gregoire CH, Goffinet G (1979) Controversies about the coagulocyte. In: Gupta AP (ed) Insect hemocytes. Cambridge University Press, Cambridge, pp 189–229

Haine ER, Rolff J, Siva-Jothy MT (2007) Functional consequences of blood clotting in insects. Dev Comp Immunol 31:456–464

Hyman LH (1959) Phylum sipunculida. In: Hyman LH (ed) The invertebrates, vol 5. McGraw-Hill, New York, pp 610–696

Jiravanichpaisal P, Lee BL, Soderhall K (2006) Cell-mediated immunity in arthropods: hematopoiesis, coagulation, melanization and opsonization. Immunobiology 211:213–236

Kristof A, Wollesen T, Wanninger A (2008) Segmental mode of neural patterning in sipuncula. Curr Biol 18:1129–1132

Kroemer G, Galluzzi L, Vandenabeele P, Abrams J, Alnemri ES, Baehrecke EH, Blagosklonny MV, El-Deiry WS, Golstein P, Green DR, Hengartner M, Knight RA, Kumar S, Lipton SA, Malorni W, Nunez G, Peter ME, Tschopp J, Yuan J, Piacentini M, Zhivotovsky B, Melino G (2009) Classification of cell death: recommendations of the Nomenclature Committee on Cell Death 2009. Cell Death Differ 16:3–11

Lavine MD, Strand MR (2002) Insect hemocytes and their role in immunity. Insect Biochem Mol Biol 32:1295–1309

McMahon BR, Smith PJS, Wilkens JL (1997) Invertebrate circulatory systems. In: Danzler WH (ed) Handbook of physiology, vol II. American Physiological Society, New York, pp 931–1008

Mitchison TJ, Cramer LP (1996) Actin-based cell motility and cell locomotion. Cell 84:371–379

Munafo DB, Colombo MI (2001) A novel assay to study autophagy: regulation of autophagosome vacuole size by amino acid deprivation. J Cell Sci 114:3619–3629

Osaki T, Kawabata S (2004) Structure and function of coagulogen, a clottable protein in horseshoe crabs. Cell Mol Life Sci 61:1257–1265

Pincus JH, Chung SI, Chace NM, Gross M (1975) Dansyl cadaverine: a fluorescent probe and marker in cell membrane studies. Arch Biochem Biophys 169:724–730

Ratcliffe NA, Gagen SJ (1977) Studies on the in vivo cellular reactions of insects: an ultrastructural analysis of nodule formation in *Galleria mellonella*. Tissue Cell 9:73–85

Rice M (1993) Sipuncula. In: Harrison FW, Rice ME (eds) Microscopic anatomy of invertebrates, vol 12: onychophora, chilopoda, and lesser protostomata. Wiley-Liss, New York, pp 237–325

Rowley AF, Ratcliffe NA (1976) The granular cells of *Galleria mellonella* during clotting and phagocytic reactions in vitro. Tissue Cell 8:437–446

Scherfer C, Karlsson C, Loseva O, Bidla G, Goto A, Havemann J, Dushay MS, Theopold U (2004) Isolation and characterization of hemolymph clotting factors in *Drosophila melanogaster* by a pullout method. Curr Biol 14:625–629

Schmidt O, Theopold U (1997) *Helix pomatia* lectin and annexin V, two molecular probes for insect microparticles: possible involvement in hemolymph coagulation. J Insect Physiol 43:667–674

Schulze A, Cutler EB, Giribet G (2007) Phylogeny of sipunculan worms: a combined analysis of four gene regions and morphology. Mol Phylogenet Evol 42:171–192

Shapiro HM (2003) Practical flow cytometry. Wiley-Liss, Hoboken, NJ

Shattil SJ, Cunningham M, Wiedmer T, Zhao J, Sims PJ, Brass LF (1992) Regulation of glycoprotein IIb-IIIa receptor function studied with platelets permeabilized by the pore-forming complement proteins C5b-9. J Biol Chem 267:18424–18431

Solum NO, Murer E (2007) Early studies on the coagulogen (clottable protein) of *Limulus polyphemus* (horseshoe crab). Thromb Haemost 98:129–130

Stossel TP (1993) On the crawling of animal cells. Science 260:1086–1094

Struck TH, Schult N, Kusen T, Hickman E, Bleidorn C, McHugh D, Halanych KM (2007) Annelid phylogeny and the status of sipuncula and echiura. BMC Evol Biol 7:57

Theopold U, Li D, Fabbri M, Scherfer C, Schmidt O (2002) The coagulation of insect hemolymph. Cell Mol Life Sci 59:363–372

Theopold U, Schmidt O, Soderhall K, Dushay MS (2004) Coagulation in arthropods: defence, wound closure and healing. Trends Immunol 25:289–294

Towle A (1975) Cell types in the coelomic fluid of *Phascolosoma agassizii*. In: Rice ME, Todorovic M (eds) Proceedings of the International Symposium on the Biology of Sipuncula and Echiura. Naunco Delo, Belgrade, pp 211-218

Triplett EL, Cushing JE, Durall GL (1958) Observations on some immune reactions of the sipunculid worm *Dendrostomum zosterticolum*. Am Nat 92:287–293

Vida TA, Emr SD (1995) A new vital stain for visualizing vacuolar membrane dynamics and endocytosis in yeast. J Cell Biol 128:779–792